

# An alternative Biot's formulation for dissipative porous media with skeleton deformation

François-Xavier Bécot<sup>a)</sup> and Luc Jaouen  
*Matelys, 1 rue Baumer, 69120 Vaulx-en-Velin, France*

(Received 30 October 2012; revised 3 October 2013; accepted 4 October 2013)

This paper presents an alternative formulation of Biot's theory to account for the elastic frame effects in a porous medium in which the acoustical properties of the fluid phase are predicted with an equivalent fluid model. This approach was originally developed for a double porosity medium. In this paper, the alternative formulation is applied to predict the transmission loss and absorption coefficient in the case of a single layer fibrous material, a multi-layer system, vibrating perforated plates, and porous composite materials. In the proposed formulation the coupling coefficients in Biot's poroelasticity equations are expressed in terms of the dynamic volumic mass and dynamic bulk modulus. By doing so, the elastic properties of the material frame are considered independently from the properties of the fluid. This formulation is implemented in the form of a transfer matrix algorithm which is validated against experimental data on sound absorption and sound transmission which are obtained for a range of various sound excitations and material arrangements. It is shown that this approach is able to predict accurately the acoustical properties of vibrating perforated plates and porous composites. The proposed approach is sufficiently general to be implemented in a finite element method. © 2013 Acoustical Society of America.

[<http://dx.doi.org/10.1121/1.4826175>]

PACS number(s): 43.55.Ev, 43.20.Jr [KVH]

Pages: 4801–4807

## I. INTRODUCTION

The acoustic performance of poroelastic materials used in sound packages is controlled by dissipative effects in the fluid filling the porous space and by the deformation of the porous skeleton. On this basis, Biot proposed a system of coupled displacement equations, one for the porous frame and one for the interstitial fluid. In this model the frame deformation is linked to the displacement of the fluid via some source terms. One of the main assumptions of Biot's approach is that the dissipation in the fluid is independent of the dissipation in the skeleton. The present work proposes to modify Biot's original theory formulations to explore this assumption further and back it up with experimental data.

It should be stressed that the proposed alternative to Biot's approach is suited to model a large range of poroelastic materials accounting for the porous frame deformation and it can make use of any fluid dissipation model, rather than rely only on the five parameter Johnson–Champoux–Allard model which is almost exclusively cited in the relevant literature. In a general manner, the fluid dissipation is represented using the dynamic mass density and the dynamic compressibility while the porous frame deformation is represented using elastic and damping parameters such as Young's modulus, Poisson's ratio, volumic mass, and loss factor. As shown in Sec. II B, the proposed method can be applied to any existing form of Biot's poro-elasticity equations. The proposed approach can include asymptotic limits of the elastic frame behavior, i.e., “rigid-body” and “limp” material approximations, see Sec. III B.

In the last part, Sec. IV, results using the actual formulation are compared with those either measured or predicted with other approaches for various materials. The materials examined here comprise single layer fibrous material, three layer system, perforated panels, and porous composites materials. Predictions using the proposed formulation are compared to measured or simulated data reported in the previous literature. These results prove that the proposed formulation allows us to reduce the number of parameters which are required to predict the acoustical properties of porous media with an elastic frame. The proposed model also enables us to consider additional physical phenomena for a deeper understanding of the dissipation mechanisms in poro-elastic materials. This feature is demonstrated for multi-scale effects occurring in porous composites.

## II. THEORETICAL BASIS OF THE PROPOSED MODEL

In this section, the theoretical basis of the proposed model is described. The purpose of this section is to show how the properties of the fluid are implemented and how one can take advantage of an appropriate rewriting of the equations.

### A. Basis assumptions

Hypotheses of Biot's theory are closely link to those of the homogenization approach for periodic media as described, for instance, in Ref. 1. The current study is limited to porous media composed of two phases, an elastic phase and a fluid phase: air. The fluid may undergo visco-inertial and thermal dissipations while the elastic phase may be subjected to structural losses.

It is assumed that the fluid fully saturates the pore volumes. The phases are continuous, which means that only

<sup>a)</sup>Author to whom correspondence should be addressed. Electronic mail: [fxb@matelys.com](mailto:fxb@matelys.com)

connected pores are considered for the visco-thermal dissipation in the fluid. The pore size distribution has a low standard deviation so that a mean value for the pore size can be used with good accuracy. The mean pore size is small compared to the wavelengths of the studied phenomena, namely, wave propagation in the fluid and that in the elastic frame. In addition, we will assume that the medium is isotropic as in the work published by Biot in 1956. In this framework, the studied medium may be considered as homogeneous at a macroscopic scale and one can define a representative elementary volume which is small compared to the wavelength of the acoustic perturbations.

It may be remembered finally that Biot's theory, originally developed for fluid saturated porous media, included the viscous effects using a tortuosity factor and neglected thermo-dynamical dissipation. This restriction could be relieved by introducing a complex valued fluid compressibility (see, for instance, Ref. 2). The present work further extends this feature by showing how to couple elastic effects to several models of visco-thermal dissipation.

## B. Formulation of the proposed model

The proposed model is presented here in the framework of the so-called  $(\mathbf{u}, p)$  formulation where  $\mathbf{u}$  is the frame displacement and  $p$  the interstitial pressure. However, this formalism may be shown to be valid for other formulations like  $(\mathbf{u}, \mathbf{U})$  (Refs. 3, 4) or  $(\mathbf{u}, \mathbf{u}')$ .<sup>5</sup> In these formulations,  $\mathbf{U}$  represents the fluid displacement and  $\mathbf{u}'$  is the total displacement defined as  $\mathbf{u}' = (1 - \phi)\mathbf{u} + \phi\mathbf{U}$ ,  $\phi$  being the porosity of the medium. This formulation expresses the fluid motion equation in terms of the interstitial pressure  $p$  and is attributed to Atalla for dedicating a communication in Ref. 6. The equations of motion can be written as

$$\nabla \cdot \sigma^s + \omega^2 \tilde{\rho} \mathbf{u} = -\tilde{\gamma} \nabla p, \quad (1)$$

$$\Delta p + \frac{\tilde{\rho}_{22}}{\tilde{R}} \omega^2 p = \frac{\tilde{\rho}_{22}}{\phi^2} \tilde{\gamma} \omega^2 \nabla \cdot \mathbf{u}, \quad (2)$$

where  $\sigma^s$  is the *in vacuo* stress tensor. In the above equations, coupling terms are written in the right hand side members. Using these expressions, the number of degrees of freedom is reduced from 6 to 4: three frame displacements and the scalar pressure, which may be of particular interest for implementation as finite element models.

In addition,  $\tilde{\rho}$  and  $\rho_{22}$  are modified Biot's densities defined below and  $\tilde{R}$  can be interpreted as the bulk modulus of a volume of fluid occupying a fraction  $\phi$  of the porous medium. The coupling factor  $\tilde{\gamma}$  is defined as

$$\tilde{\gamma} = \phi \left( \frac{\tilde{\rho}_{12}}{\tilde{\rho}_{22}} - \frac{\tilde{Q}}{\tilde{R}} \right). \quad (3)$$

Some of these coefficients are related to the coupling between the elastic effects and the fluid properties,

$$\tilde{Q} = \frac{\left[ 1 - \phi - \frac{K_b}{K_s} \right] \phi K_s}{D}, \quad (4)$$

$$\tilde{R} = \frac{\phi^2 K_s}{\tilde{D}}, \quad (5)$$

with

$$\tilde{D} = 1 - \phi - \frac{K_b}{K_s} + \frac{K_s}{\tilde{K}_{eq}}, \quad (6)$$

where  $K_b$  is the bulk modulus of the frame at constant pressure in air and  $K_s$  is the bulk modulus of the elastic material from which the porous frame is made.

The other coefficients depend exclusively on the fluid properties or on the pore geometry. Biot's modified mass densities are expressed as

$$\tilde{\rho}_{22} = \phi^2 \tilde{\rho}_{eq}, \quad (7)$$

$$\tilde{\rho}_{12} = \phi \rho_0 - \tilde{\rho}_{22}, \quad (8)$$

$$\tilde{\rho}_{11} = \rho_1 - \tilde{\rho}_{12}, \quad (9)$$

$$\tilde{\rho} = \tilde{\rho}_{11} - \frac{\tilde{\rho}_{12}^2}{\tilde{\rho}_{22}}. \quad (10)$$

$\rho_1$  is the volumic mass of the frame and can be calculated by  $\rho_1 = (1 - \phi)\rho_s$  where  $\rho_s$  is the volumic mass of the solid constituting the frame.  $\rho_0$  is the volumic mass of the air at rest.

Therefore, the coefficients of the above Biot's poroelasticity equations can be expressed as

$$\tilde{\rho} = \rho_1 + \phi \rho_0 - \frac{\rho_0^2}{\rho_{eq}}, \quad (11)$$

$$\tilde{\gamma} = \frac{\rho_0}{\rho_{eq}} - 1 + \frac{K_b}{K_s}, \quad (12)$$

$$\tilde{\rho}_{22} = \phi^2 \tilde{\rho}_{eq}, \quad (13)$$

$$\tilde{R} = \frac{\phi^2 K_s}{\tilde{D}} = f(\tilde{K}_{eq}), \quad (14)$$

where  $f$  is some analytic function of the frequency  $\omega$ .  $\tilde{\rho}_{eq}$  and  $\tilde{K}_{eq}$  are, respectively, the dynamic mass density and the bulk modulus of the porous material.  $\tilde{\rho}_{eq}$  is associated with visco-inertial effects and  $\tilde{K}_{eq}$  is associated with thermal dissipative effects. A large number of expressions exist in literature for these two quantities depending on the dissipative models selected.<sup>7-11</sup>

At this point, one could note that for most porous materials found in vibro-acoustic applications, the bulk modulus  $K_s$  of the material constituting the elastic frame is much larger than that of the material itself  $K_b$ . In addition, the bulk modulus of the saturating air,  $K_f = \phi \tilde{K}_{eq}$ , is much less than that of the material  $K_s$ . For most sound proofing materials,  $\phi$  is close to 1, and thus  $\tilde{K}_{eq}$  is still much lower than  $K_s$ .

Using these assumptions, the coefficients may be further simplified to be written in the following form:

$$\tilde{\rho} = \rho_1 + \phi \rho_0 - \frac{\rho_0^2}{\rho_{eq}}, \quad (15)$$

$$\tilde{\gamma} = \frac{\rho_0}{\rho_{eq}} - 1, \quad (16)$$

$$\widetilde{\rho}_{22} = \phi^2 \widetilde{\rho}_{\text{eq}}, \quad (17)$$

$$\widetilde{R} = \phi^2 \widetilde{K}_{\text{eq}}. \quad (18)$$

Finally, Eqs. (1) and (2) can be written in a more explicit form as

$$\nabla \cdot \boldsymbol{\sigma}^s + \omega^2 \left( \rho_1 + \phi \rho_0 - \frac{\rho_0^2}{\rho_{\text{eq}}} \right) \mathbf{u} = - \left( \frac{\rho_0}{\rho_{\text{eq}}} - 1 \right) \nabla p, \quad (19)$$

$$\Delta p + \frac{\rho_{\text{eq}}}{K_{\text{eq}}} \omega^2 p = \widetilde{\rho}_{\text{eq}} \left( \frac{\rho_0}{\rho_{\text{eq}}} - 1 \right) \omega^2 \nabla \cdot \mathbf{u}. \quad (20)$$

The key originality of this approach is that, for all formulations reported here, the models for the fluid dissipation is inherently contained in the quantities  $\widetilde{\rho}_{\text{eq}}$  and  $\widetilde{K}_{\text{eq}}$ . Therefore, any existing equivalent fluid model can be used to predict the values of these quantities. More precisely, this means that the model could be chosen on a various range of criteria, e.g., on the basis of the parameters which are available, prior knowledge of the material behavior, and required complexity of the material modeling approach. These aspects will be discussed further in the next section.

### III. EQUIVALENT FLUID PROPERTIES

The derivations of the preceding section demonstrate that two independent sets of parameters are required to implement the poro-elasticity equations following Biot's formulation: the parameters related to the elastic behavior of the skeleton and those related to the visco-thermal dissipation inside the fluid phase. This current section focus on the visco-thermal modeling.

#### A. Dynamic properties

As a general principle, the propagation of sound in a fluid medium is fully described by wave impedance and a wavenumber. For sound propagating in air without dissipation, these quantities are independent of the frequency of excitation. Their values are  $Z_c = \rho_0 c_0$  and  $k_c = \omega/c_0$ , where  $\rho_0$  and  $c_0$  are, respectively, the volumic mass of air and the sound speed in air. These two phenomena are highly dependent on the wavelength of the acoustic perturbation. Thus, it shall be represented by dynamic quantities which depend on frequency,  $Z_c(\omega)$  and  $k_c(\omega)$ . These two latter quantities are related to the dynamic volumic mass and bulk modulus of a porous medium by

$$Z_c(\omega) = \sqrt{\widetilde{\rho}_{\text{eq}} \widetilde{K}_{\text{eq}}} \quad \text{and} \quad k_c(\omega) = \omega \sqrt{\frac{\widetilde{\rho}_{\text{eq}}}{\widetilde{K}_{\text{eq}}}}. \quad (21)$$

It should be underlined that these two quantities may be computed independently. Depending on the type of materials, they may be expressed differently and according to various micro-structural parameters.

In addition, the coupling with the full Biot's poroelasticity equations implies that the considered elastic deformations

cope with thick plate theories. This aspect will be particularly interesting when studying the deformation of perforated plates which do not necessarily fulfill Mindlin theory (see Sec. IV B). This formulation also copes with orthotropic or anisotropic solid plate theories, see, e.g., Ref. 12 and anisotropic formulation dedicated to porous materials, e.g., Refs. 13, 14. However, this feature will not be investigated in the present paper.

#### B. The particular cases of limp and rigid body behaviors

The above equations describe the visco-inertial dissipation in a porous medium with a rigid and motionless frame. Sound propagation can then be modeled with the Helmholtz equation for the interstitial pressure. This equation can be written in the following form:

$$\Delta p + \omega^2 \frac{\widetilde{\rho}_{\text{eq}}}{K_{\text{eq}}} p = 0. \quad (22)$$

To overcome the limitations of a rigid and motionless frame, expression of the complex mass density  $\widetilde{\rho}_{\text{eq}}$  may be modified to improve the description of inertial effects. Two hypotheses are available for this: (i) the material moves as a whole without deforming and (ii) the porous skeleton is so soft that the coupling between the frame and the interstitial fluid is weak. These two limit cases are often referred to as, respectively, the "rigid body" hypothesis and "limp" hypothesis.

The first case is relevant to those situations where the ratio of the Young's modulus to volumic mass density is high. This situation may be encountered for stiff materials, though with a low mass density. In this case, the porous frame does not deform but inertial effects may occur because the porous material is allowed to move in a rigid body motion. Starting from Biot's poroelasticity equations, see Eqs. (1) and (2), this situation corresponds to  $\nabla \cdot \mathbf{u} = 0$ . After some algebraic manipulations, the complex mass density can be expressed with<sup>15</sup>

$$\frac{1}{\widetilde{\rho}_{\text{eq}}^{\text{RB}}} = \frac{1}{\phi \widetilde{\rho}_{\text{eq}}} + \frac{\gamma^2}{\phi \widetilde{\rho}} + \frac{(1-\phi)\gamma}{\phi \widetilde{\rho}}. \quad (23)$$

The second case, the limp hypothesis, is most known in the community. This corresponds to situations where the ratio Young's modulus to volumic mass density is small. Typical examples of limp materials are soft, highly porous fibrous materials. In this case, the bulk modulus  $K_b$  and the shear modulus  $N$  are assumed to have zero values. Some algebraic manipulations of Biot's equations lead to the following expression of the modified complex mass density for the limp case:<sup>15-17</sup>

$$\frac{1}{\widetilde{\rho}_{\text{eq}}^{\text{limp}}} = \frac{1}{\phi \widetilde{\rho}_{\text{eq}}} + \frac{\gamma^2}{\phi \widetilde{\rho}}. \quad (24)$$

This hypothesis has been proved to lead to accurate, computationally more efficient models which can be used in

the situation where the porous materials are not directly coupled to a vibrating structure.<sup>15,18</sup>

From the two above equations, it is obvious that for highly porous materials ( $\phi \approx 1$ ) which are often studied in vibro-acoustic problems, the two hypotheses lead to the same expression for the mass density. Therefore in the following, only the limp hypothesis will be examined. One should keep in mind however that, e.g., for stiff semi-closed cell foams having low open porosity, the two hypotheses may lead to significant differences at low frequencies.

#### IV. EXPERIMENTAL VALIDATIONS

This section presents three configuration examples where the proposed formalism is compared to measured data or simulations available in literature. These comprise the prediction of diffuse field absorption coefficients using a one-parameter model, diffuse field sound transmission loss of vibrating perforated panels, and deformable porous composite materials. Results are compared with data extracted from literature or measured by the authors. In all these examples, predicted results have been obtained using an in-house TMM software.

##### A. Calculations with one parameter models

The present section illustrates situations where the model should be adapted to the available parameters for the tested material. In the two examples below, it is assumed that only the static air flow resistivity  $\sigma$  is available. Therefore, the model used is the so-called Delany–Bazley–Miki (DBM) model which corresponds to the well-known Delany–Bazley model<sup>19</sup> further modified by Miki<sup>20</sup> to fulfill physical causality of the predicted surface impedance. The domain of validity of this latter model is said to be the same as the original Delany–Bazley model, namely,  $0.01 < f/\sigma < 1.00$ . This would yield a lower frequency limit of around 350 Hz. It may also be pointed out that Miki also observed that the revised expressions are well behaved in a larger frequency range, in particular for  $f/\sigma < 0.01$ , which corresponds to a lower frequency limit of the model validity. Therefore, it is expected that the model proposed here is valid on most of the frequency range observed here, i.e., from 100 to 5000 Hz. For the elastic effects, two implementations are shown in each case. Either the full Biot’s poroelasticity equations are used or a limp hypothesis is assumed.

In the first example the prediction of the diffuse field sound absorption is compared against reverberant chamber data. The diffuse field condition is modeled by integrating all incidence angles from normal incidence to grazing incidence. A single layer of material is directly laid onto an acoustically rigid floor. The one-parameter DBM model is used together with measured data that are extracted from Ref. 21 [Chap. 12, Fig. 12.8]. Note that since the tested material slabs are relatively small, a finite size correction should be applied. Because samples have a square shape, the correction model proposed by Vigran<sup>22</sup> was applied in this study.

A comparison between measured and predicted results is shown in Fig. 1. The two sets of predictions compare well with measured data for the frequencies above 400 Hz. Below

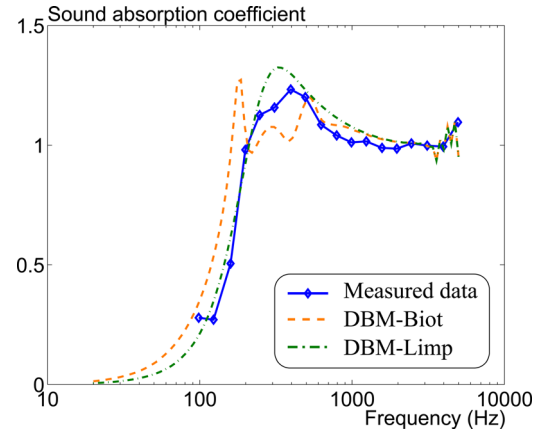


FIG. 1. (Color online) Sound absorption coefficient of  $6 \times 6$  ft foam samples: Comparison between measured data ( $\diamond$ ) and numerical prediction. - - -: DBM model with structural effects; - · - ·: DBM model with limp assumptions.

this frequency the predictions by Biot’s theory show a peak at around 200 Hz which is not observed in the measurements. In this case, the limp model captures better the observed behavior. This may be due to the fact that the material slab is not constrained on its perimeter, thus decreasing the effect of structural resonances at low frequencies.

The second example concerns the prediction of the diffuse field sound transmission for a double leaf partition consisting of a laminate and a steel plate between which a heavy mineral wool ( $90 \text{ kg m}^{-3}$ ) is being sandwiched. This configuration is extracted from Ref. 23 (Fig. 16) where the material properties for each component can be found. Here again, a finite size correction according to the Vigran’s algorithm has been applied.<sup>22</sup> Simulated and measured results are compared in Fig. 2. They show that the two sets of predictions agree well with the measured data at frequencies above 500 Hz. The resonance observed at this frequency corresponds to a breathing frequency of the double-leaf system. At lower frequencies, the finite size correction allows us to capture correctly the increased sound transmission loss due to the finite size of the tested system.

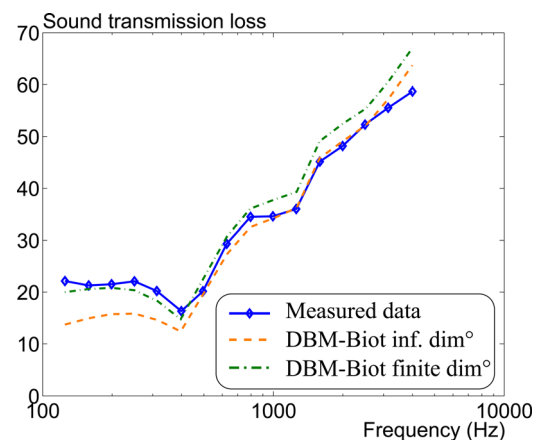


FIG. 2. (Color online) Sound transmission loss of a multi-layer system: comparison between measured data ( $\diamond$ ) and numerical prediction. - - -: Miki model for laterally infinite sample; - · - ·: Miki model for a finite size sample using Vigran approach.



At higher frequencies, consistent differences are also observed between the TMM and the FTMM results. This deviation is also observed in the results of the original paper.<sup>23</sup> In fact, the finite size correction is expected to influence the results up to the critical frequency of the studied material. In our case, two critical frequencies corresponding to the two different panel types may be observed. These critical frequencies lie around 16 kHz for the steel plate and above 32 kHz for the laminate. Therefore, the impact of the FTMM correction is observed here for the entire frequency range studied.

## B. Vibrating perforated panel

Another range of applications where the proposed formalism may be efficiently implemented concerns the vibrating behavior of perforated panels. The model presented in this section is based on the work by Atalla and Sgard<sup>24</sup> which described the visco-thermal dissipation inside arbitrarily shaped perforations. It is proposed here to account for the plate vibration using Biot's formalism as described above.

Experimental and numerical data are extracted from Ref. 25 where the reader will find the complete description of the two configurations studied here. In the two cases, the dissipation inside the perforations is described using the five-parameter model, which is usually referred to as Johnson–Champoux–Allard model.<sup>8,26</sup> This models makes use of the static air flow resistivity  $\sigma$ , which may be analytically calculated for simple shape perforations, the porosity  $\phi$ , which corresponds to the perforation rate  $\phi_p$  defined as the volume of the perforations to the total sample volume, the viscous and thermal characteristic lengths,  $\Lambda$  and  $\Lambda'$ , which in this particular case are equal and correspond to the hydraulic radius, and  $\alpha_\infty$ , which is the high frequency limit of the dynamic tortuosity whose value depends on the morphology of the perforation and on the nature of the adjacent layers.<sup>24</sup>

Comparisons are shown in Fig. 3 for sound transmission performances and in Fig. 4 for sound absorption results. In the case of the sound transmission, the predictions compare

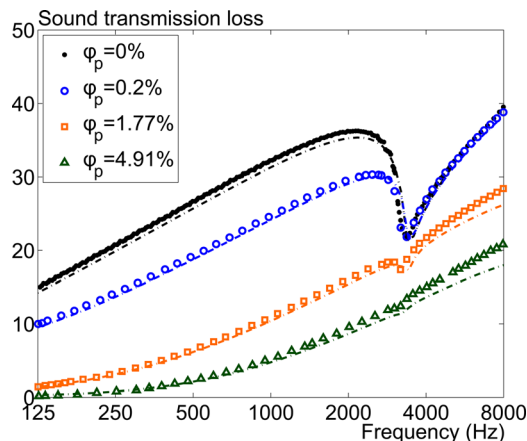


FIG. 3. (Color online) Sound transmission loss of a solid perforated panel with different perforation rate  $\phi_p$ ; comparison between prediction from Ref. 25 [Fig. 4(b)] (●, ○, □, △) and numerical prediction (---).

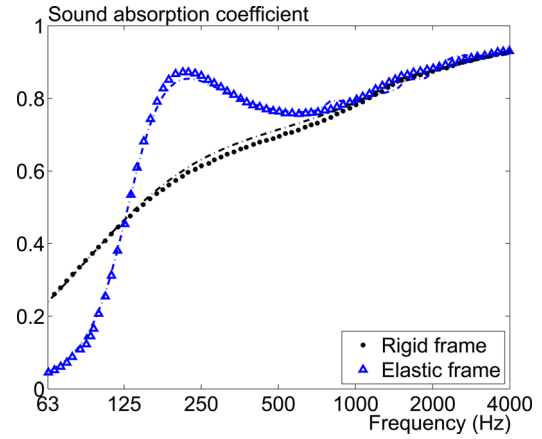


FIG. 4. (Color online) Sound absorption coefficient of a poro-elastic plate backed with a 100 mm air gap. Comparison between prediction from Ref. 25 (Fig. 7) (symbols) and numerical prediction (broken lines). Rigid frame assumption: ●, ---; elastic frame assumption: △, ---.

well with the reference data for all perforation rates examined here. Note that for the  $\phi_p = 0\%$  configuration, the present formalism using Biot's theory corresponds to the classical three dimensional plate elasticity theory. For sound absorption configurations, the proposed formalism allows us to capture the significant increase of performance in the low frequency range.

## C. Deformable porous composites

The last series of examples concerns the modeling of porous composites consisting of a macro-perforated porous material hosting a foreign porous inclusion. For the material considered here, the geometry of the inclusion is a cylinder which diameter fits tightly the perforation cut in the host material. The viscous and thermal permeabilities of the fluid are expressed, respectively, from a general mixing law as<sup>27</sup>

$$\Pi_{PC} = \phi_p \Pi_C + (1 - \phi_p) \Pi_H, \quad (25)$$

$$\Theta_{PC} = \phi_p \Theta_C + (1 - \phi_p) \Theta_H F_d, \quad (26)$$

where the subscript PC stands for porous composite,  $H$  and  $C$ , respectively, for host and client materials, and  $F_d$  is the pressure diffusion function which expression can be found in Ref. 28. The two sets of permeabilities are defined from the properties of the constituting porous materials, respectively, by

$$\Pi_i = \frac{\eta_0}{j \rho_{eq_i}}, \quad (27)$$

$$\Theta_i = \frac{k'_{0i}}{j\omega \frac{\rho_0 C_p k'_{0i}}{\kappa \phi_i} + \left(1 + \frac{j}{2} \frac{8\kappa}{\rho_0 C_p \Lambda_i^2}\right)^{1/2}}, \quad (28)$$

where  $i = C$  or  $H$ . Then, the dynamic volumic mass and compressibility are calculated using standard relationships as

$$\tilde{\rho}_{PC} = \frac{\eta_0}{j \Pi_{PC}}, \quad (29)$$

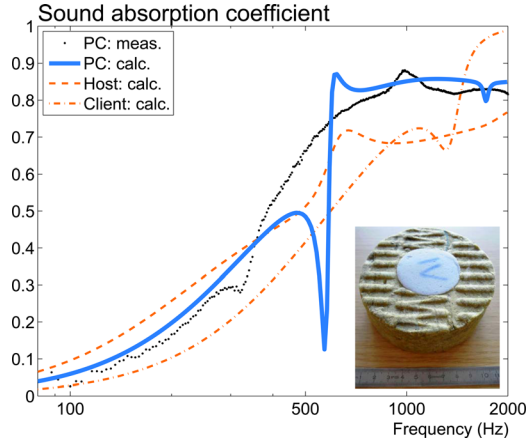


FIG. 5. (Color online) Sound absorption coefficient of a porous composite (PC) material made from a perforated rock wool (host) and a melamine inclusion (client). Comparison between measured data ( $\cdots$ ) and numerical prediction ( $\text{—}$ ). Calculation for host alone:  $\text{- - -}$  and for client alone:  $\text{- \cdot -}$ .

$$\tilde{K}_{PC} = \frac{\gamma P_0 / \phi_{PC}}{\gamma - j(\gamma - 1)\Theta_{PC} / \phi_{PC}\kappa}. \quad (30)$$

$\gamma$  is the ratio of the specific heats,  $\kappa$  is the thermal conductivity of the saturating air, and  $P_0$  is the atmospheric pressure. Here  $\phi_{PC}$  is the total porosity of the porous composite calculated as  $\phi_{PC} = \phi_p \phi_C + (1 - \phi_p)\phi_H$  where  $\phi_p$  is the rate of inclusion, also called meso-porosity in double porosity theory. It also corresponds to the perforation rate introduced in the previous example.

On the other hand, the effective elastic properties are calculated from a self-consistent approach for a cylindrical inclusion in a circular sample.<sup>29</sup> For this geometry, derivation of the exact expressions of Young's modulus and Poisson's ratio exist and can be found in Ref. 30. Expressions are quite lengthy and only the expressions of the longitudinal Young's modulus and the longitudinal Poisson's ratio are given below as examples,

$$E_L = E_C \phi_p + E_H (1 - \phi_p) + \cdots, \quad (31)$$

$$\frac{4(\nu_C - \nu_H)^2 \phi_p (1 - \phi_p)}{\phi_p / K_H + (1 - \phi_p) / K_C + 1 / G_H}, \quad (32)$$

$$\nu_{LT} = \nu_C \phi_p + \nu_H (1 - \phi_p) + \cdots, \quad (33)$$

$$\frac{(\nu_C - \nu_H) \phi_p (1 - \phi_p) (1 / K_H - 1 / K_C)}{\phi_p / K_H + (1 - \phi_p) / K_C + 1 / G_H}. \quad (34)$$

$K_H$  and  $K_C$  are the lateral compression moduli and  $G_H$  is shear modulus for the host material. In addition, the mass

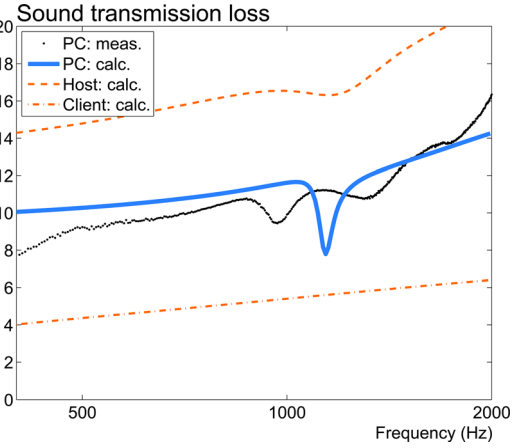


FIG. 6. (Color online) Sound transmission loss of a porous composite (PC) material made from a perforated rockwool (host) and a melamine inclusion (client). Comparison between measured data ( $\cdots$ ) and numerical prediction ( $\text{—}$ ). Calculation for host alone:  $\text{- - -}$  and for client alone:  $\text{- \cdot -}$ .

density and the structural loss factor of the porous composite are given using a mixing law as

$$\rho_{1,PC} = \phi_p \rho_{1,C} + (1 - \phi_p) \rho_{1,H}, \quad (35)$$

$$\eta_{PC} = \phi_p \eta_C + (1 - \phi_p) \eta_H. \quad (36)$$

This model therefore requires the acoustic, elastic, and damping parameters of the two material components separately. For the material considered here (see also inset in Fig. 5), the host material is heavy stone wool and the client is melamine foam. The parameters for these two materials have been characterized at Matelys and are reported in Table I.

Sound absorption coefficient and sound transmission loss have been measured in a 100 mm diameter impedance tube following ISO 10534-2.<sup>31,32</sup> Measured data are compared to the simulation obtained using the porous composite model described above. In addition, calculation of the properties of the host and of the client alone are also reported. Results are shown in Fig. 5 for the sound absorption and in Fig. 6 for the sound transmission.

In these graphs, the measured data show rapid variations due to elastic deformation of the porous skeleton around 300 and 1000 Hz. It is observed that the model for the porous composites predicts this phenomenon in a higher frequency range than that observed in the measured data. The reason is that the frequency at which this phenomenon occurs largely depends on the mounting conditions of the sample inside the tube, conditions which are not accurately known. Besides these deviations, the general behavior is correctly captured for both the absorption and the transmission properties of the

TABLE I. Acoustic, elastic, and damping parameters of the host and client materials constituting the porous composite.

Material	$\sigma$	$\phi$	$\alpha_\infty$	$\Lambda$	$\Lambda'$	$k'_0$	$E$	$\eta$	$\nu$	$\rho_1$
Host	88 400	0.97	1.01	19	48	10	1375	0.3	0	160
Client	15 500	0.98	1.01	100	223	27	200	0.1	0.42	11
Units	N s m <sup>-4</sup>	—	—	$\mu\text{m}$	$\mu\text{m}$	10 <sup>-10</sup> m <sup>2</sup>	kPa	—	—	kg m <sup>-3</sup>

porous composite. Comparisons with the predictions for the host and for the client materials alone illustrate the need of this type of model which reproduces the modification of the acoustic and of the elastic properties of the resulting heterogeneous material.

## V. CONCLUSION

This paper presents an alternative formalism based on Biot's theory which allows one to account for structural effects with a majority of the existing equivalent fluid models for the acoustical properties of porous media. Structural effects are related to the deformation of the solid phase of the material whereas the visco-inertial and thermal dissipation is associated with the wave propagation in the interstitial fluid of the porous material.

The proposed approach relies on the assumption made by Biot that the dissipation in the fluid phase is independent of the dissipation which may occur in the material skeleton. It is highlighted that the proposed formalism applies to various derivations of Biot's poroelasticity equations. Therefore, the model for the fluid phase may be selected according to the information which is available for the material, provided that this information is sufficient to describe the material behavior.

The proposed model has been used in three types of simulations. The first type relates to the problem of modeling sound absorption and sound transmission using a single parameter model. The second type relates to the problem of predicting the vibro-acoustic response of perforated panels accounting for the panel deformation. The third type relates to the problem of modeling structural effects in porous composite materials.

For the simulations using a single parameter model, predictions obtained using the proposed model agree well with measured data and with predictions using other forms of Biot's poroelasticity equations. For the problem of modeling vibrating perforated plates, the agreement with a classical fluid-structure interaction model is good for several perforation rates. Finally, for porous composites, comparisons with measured data obtained using the impedance tube show that the proposed model allows one to capture the correct trend at both low and high frequencies. For the medium frequency range, resonance effects due to the porous frame deformation are not correctly reproduced as the exact boundary conditions on the sample circumference are not known. Improving the accuracy of the TMM algorithm to include various types of boundary conditions is subject to ongoing work.

<sup>1</sup>E. Sanchez-Palencia, *Non-homogeneous Media and Vibration Theory* (Springer Verlag, Berlin, 1980).

<sup>2</sup>C. Zwikker and W. Kosten, *Sound Absorbing Materials* (Elsevier, New York, 1949).

<sup>3</sup>M. A. Biot, "Theory of propagation of elastic waves in a fluid-saturated porous solid. I. Low-frequency range," *J. Acoust. Soc. Am.* **28**, 168–178 (1956).

<sup>4</sup>M. A. Biot, "Theory of propagation of elastic waves in a fluid-saturated porous solid. II. Higher frequency range," *J. Acoust. Soc. Am.* **28**, 179–191 (1956).

<sup>5</sup>O. Dazel, B. Brouard, C. Depollier, and S. Griffiths, "An alternative Biot's displacement formulation for porous materials," *J. Acoust. Soc. Am.* **121**, 3509–3516 (2007).

<sup>6</sup>N. Atalla, R. Panneton, and P. Debergue, "A mixed displacement-pressure formulation for poroelastic materials," *J. Acoust. Soc. Am.* **104**, 1444–1452 (1998).

<sup>7</sup>A. Attenborough, "Acoustical characteristics of rigid fibrous absorbents and granular materials," *J. Acoust. Soc. Am.* **73**, 785–799 (1983).

<sup>8</sup>Y. Champoux and J.-F. Allard, "Dynamic tortuosity and bulk modulus in air-saturated porous media," *J. Appl. Phys.* **70**, 1975–1979 (1991).

<sup>9</sup>M. R. Stinson and Y. Champoux, "Propagation of sound and the assignment of shape factors in model porous materials having simple pore geometries," *J. Acoust. Soc. Am.* **91**, 685–695 (1992).

<sup>10</sup>D. Lafarge, P. Lemarinier, J.-F. Allard, and V. Tarnow, "Dynamic compressibility of air in porous structures at audible frequencies" *J. Acoust. Soc. Am.* **102**, 1995–2006 (1997).

<sup>11</sup>D. K. Wilson, "Simple, relaxational models for the acoustical properties of porous media," *Appl. Acoust.* **50**, 171–188 (1997).

<sup>12</sup>E. A. Skelton and J. H. James, "Acoustics of anisotropic planar layered media," *J. Sound Vib.* **152**, 157–174 (1992).

<sup>13</sup>S. Gorog, R. Panneton, and N. Atalla, "Mixed displacement-pressure formulation for acoustic anisotropic open porous media," *J. Appl. Phys.* **82**, 4192–4196 (1997).

<sup>14</sup>P. Khurana, L. Boeckx, W. Lauriks, P. Leclaire, O. Dazel, and J.-F. Allard, "A description of transversely isotropic sound absorbing porous materials by transfer matrices," *J. Acoust. Soc. Am.* **125**, 915–921 (2009).

<sup>15</sup>F.-X. Bécot and F. Sgard, "On the use of poroelastic materials for the control of the sound radiated by a cavity backed plate," *J. Acoust. Soc. Am.* **120**, 2055–2066 (2006).

<sup>16</sup>H.-Y. Lai, "Modeling of acoustical properties of limp fibrous materials," Ph.D. thesis, Purdue university (1997).

<sup>17</sup>R. Panneton, "Comments on the limp frame equivalent fluid model for porous media," *J. Acoust. Soc. Am.* **122**, EL217–EL222 (2007).

<sup>18</sup>N. Atalla and R. Panneton, "The effects of multilayer sound-absorbing treatments on the noise field inside a plate backed cavity," *Noise Control Eng. J.* **44**, 235–243 (1996).

<sup>19</sup>E. Delany and E. N. Bazley, "Acoustical properties of fibrous absorbent materials," *Appl. Acoust.* **3**, 105–116 (1970).

<sup>20</sup>Y. Miki, "Acoustical properties of porous materials—Modifications of Delany-Bazley models," *J. Acoust. Soc. Jpn. (E)* **11**, 19–24 (1990).

<sup>21</sup>J. Allard and N. Atalla, *Propagation of Sound in Porous Media: Modelling Sound Absorbing Materials* (Wiley, Chichester, 2009), Chap. 12, Fig. 12.8.

<sup>22</sup>T. E. Vigran, "Predicting the sound reduction index of finite size specimen by a simplified spatial windowing technique," *J. Sound Vib.* **325**, 507–512 (2009).

<sup>23</sup>M. Villot, C. Guigou, and L. Gagliardini, "Predicting the acoustical radiation of finite size multi-layered structures by applying spatial windowing on infinite structures," *J. Sound Vib.* **245**, 433–455 (2001).

<sup>24</sup>N. Atalla and F. Sgard, "Modeling of perforated plates and screens using rigid frame porous models," *J. Sound Vib.* **303**, 195–208 (2007).

<sup>25</sup>D. Takahashi and M. Tanaka, "Flexural vibration of perforated plates and porous elastic materials under acoustic loading," *J. Acoust. Soc. Am.* **112**, 1456–1464 (2002).

<sup>26</sup>D. L. Johnson, J. Koplik, and R. Dashen, "Theory of dynamic permeability and tortuosity in fluid-saturated porous media," *J. Fluid Mech.* **176**, 379–402 (1987).

<sup>27</sup>F.-X. Bécot, L. Jaouen, and F. Chevillotte, "Analytical modeling of deformable porous composites," in *Proceedings of Forum Acusticum 2011*, Aalborg, Denmark (2011).

<sup>28</sup>X. Olyny and C. Boutin, "Acoustic wave propagation in double porosity media," *J. Acoust. Soc. Am.* **114**, 73–89 (2003).

<sup>29</sup>R. M. Christensen and K. H. Lo, "Solutions for effective shear properties in three phase sphere and cylinder models," *J. Mech. Phys. Solids* **27**, 315–330 (1979).

<sup>30</sup>J.-M. Berthelot, *Materiaux Composites: Comportement Mécanique et Analyse des Structures (Composite Materials: Mechanical Behavior and Structure Analysis)* (Tec & Doc Lavoisier, Cachan, 2005).

<sup>31</sup>EN ISO 10534-2, *Acoustics—Determination of Sound Absorption Coefficient and Impedance in Impedance Tubes—Part 2: Transfer-function Method* (International Organization for Standardization, Geneva, 1991).

<sup>32</sup>J. Y. Chung and D. A. Blaser, "Transfer function method of measuring induct acoustic properties. I. Theory," *J. Acoust. Soc. Am.* **68**, 907–913 (1980).